JOURNAL OF MATERIALS SCIENCE 19 (1984) 297–302

Vickers micromechanical indentation of $BaMoO_4$ crystals

S. K. ARORA, G. S. TRIVIKRAMA RAO, N. M. BATRA
Department of Physics, Sardar Patel University, Vallabh Vidyanagar 388 120, Gujarat, India

Vickers microhardness measurements have been carried out on flux-grown single crystals of barium molydate. The dependence of hardness on indentation load, and anisotropy in hardness in the (011) and (001) planes have been described. Attempts have also been made to understand the nature of the cracks developed around the micro-indentation.

1. Introduction

Many investigations have been undertaken to correlate the indentation hardness with other physical properties. Bückle [1, 2], for instance, has pointed to the possibility of investigating various material properties by means of microhardness measurements. Although the mechanism of deformation during indentation is not clearly understood, hardness testing provides useful information concerning the mechanical behaviour of brittle solids. Several investigators [3–7] have used indentation techniques to study glide, deformation anisotropy, cracks, etc. in various crystals. The indentation is generally carried out using sharp indenters such as a cone or pyramid, because of the geometrical similarity of the residual impression [8]. The contact pressure with such a geometry is independent of indent size and thus affords a convenient measure of hardness. The Vickers hardness test method is one of the most common and reliable methods for hardness measurements. A literature survey has revealed that there has been little study of crack patterns and hardness variations for non-cubic crystals. Single crystals of tetragonal barium molybdate have been successfully grown for a study of various properties using an isothermal flux evaporation technique in this laboratory [9]. They crystallize in the well known scheelite structure, with bipyramidal and platey habits, belonging to the space group $I\,4_{1/a}$ [10]. The crystals were characterized by X-ray diffraction, energy dispersive analysis of X-rays (EDAX) and electrical properties [11, 12]. Since practically no information is available on their micromechanical behaviour, a systematic study of the hardness characteristics of these crystals was undertaken. The data so obtained are given and discussed in this paper.

2. Experimental details

The microhardness of the crystals was determined by subjecting their prominent as-grown, smooth (011) faces and also their (001) cleavage planes, to static indentation tests in air at room temperature (27° C), using the microhardness tester M06270 manufactured by Vickers Ltd, UK. The indenter orientation was fixed throughout the measurements along the ⟨100⟩ direction with respect to the planes studied. Diagonal lengths of the indented impressions obtained at various applied loads were measured using the filar micrometer of the Vickers projection metallurgical microscope. Loads, L, varying from 20 to 140 g were applied over a fixed interval of time, say 30 sec. In another set of experiments, keeping the load constant, the indentation time, t, was varied from 10 to 120 sec. Performing 10 trials of indentations for each loading, the mean value of the diagonal lengths was found. Then, following the concept of Onitsch [13], the Vickers hardness number, VHN, was calculated using the relation:

$$\mathrm{VHN} = 1.854 a d^{n-2} \quad (1)$$

0022–2461/84 $03.00 + .12

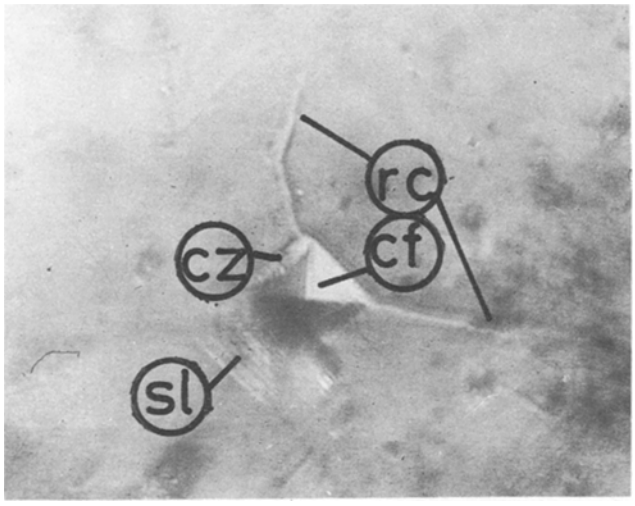

Figure 1 Typical Vickers indentation mark on a (011) face at 20 g load, exhibiting radial cracks (rc), band of cracks (cz), slip lines (sl), and crack free zone (cf) (× 730).

where a and n are constants for a given material and the environment, and d is the average diagonal length of the Vickers impression, measured in mm, after unloading. In addition the indentation-induced cracks were also examined using the filar micrometer eye piece.

3. Results and discussion

During the routine examination of Vickers indentation on the as-grown (011) and cleaved (001) planes, interesting crack patterns were observed as shown in Figs. 1, 2 and 3. It is believed that as the Vickers indenter load is increased, there occurs a transition from the purely inelastic deformation to the formation of penny-shaped cracks beneath and across the major diagonals of the Vickers indent. Subsequent loading causes these cracks to extend and cut the free surface to yield the cracks, as observed. In the case of (011) planes (Figs. 1 and 2), the slip lines (sl) in addition to the prominent crack patterns, are observed even at low load (20 g) indents. The absence of any bulk median cracks on these planes indicates the low damage done to the surface. However, the radial cracks (rc) formed along the major diagonals or the edges of the Vickers indent, when the system is not overloaded, are probably the result of the unloading residual stresses [14, 15]. Also these radial cracks, or the so called "Palmqvist cracks" [16–18], are usually confined to a narrow zone on the specimen surface, as observed. These cracks emanate from the corners of the indentation and probably do not extend beneath the deformed zone. It is known that loading

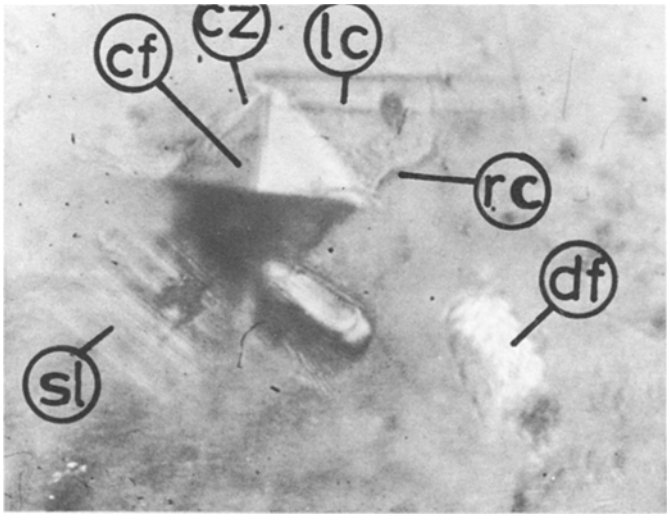

Figure 2 The indentation mark at 60 g load on a (011) face with the crack system. Note also the dislodged fragment (df) and lateral cracks (lc) in reflected light (× 680).

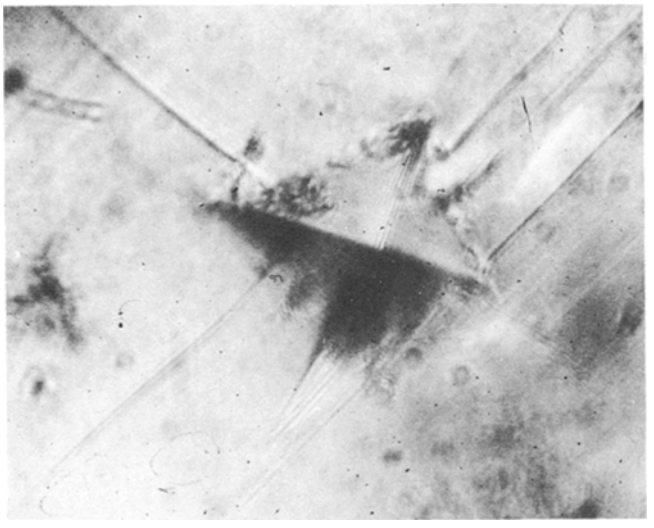

Figure 3 The typical pyramid indent at 100 g on a (001) face, showing bulk cracks in and around the indentation mark (× 790).

produces penny-like normal vents or cracks which on unloading begin to close up owing to the compressive forces of the elastically deformed material about the indentation site [14, 15]. On the surface, the elastic stresses are reversed and radial cracks are formed, which may occasionally be an extension of the surface median cracks. Our understanding of the events occurring in the deformed zone is very small. Nonetheless, with a view to quantifying these cracks, we measured the extent of cracking against indentation dwell time at different loads. The resulting variation is shown in Fig. 4, establishing that the size of the indentation is proportional to the extent of cracking. It is also revealed that the crack velocity (measured by the slope of the straight lines in Fig. 4) remains constant beyond 80 g. This nonvariation of crack velocity with load (> 80 g) may be due to non-extension of radial cracks beneath the deformed zone. It may be noted that the extent of cracking against indenter load, as depicted in Fig. 5, is reasonably linear. That the straight lines in the present case do not have an intercept on the load axis suggests reinforcement of the fact that the indentation always produces cracks even at the lightest load. This, of course, implies no significant densification due to material erosion about the indentation site on the as-grown faces. This is contrary to what has been observed for soda-lime glass [15]. Interestingly, we also observed some shallow lateral cracks (lc) on the specimen surface, which develop during or after complete unloading of the indenter [14, 19]. Since the state of stress about

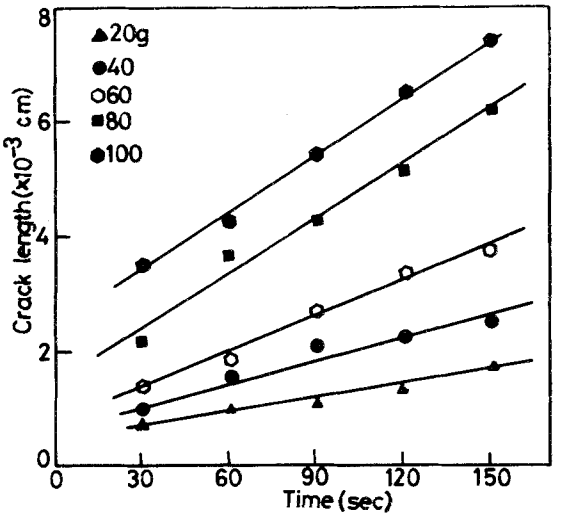

Figure 4 Plots of crack length against propagation time.

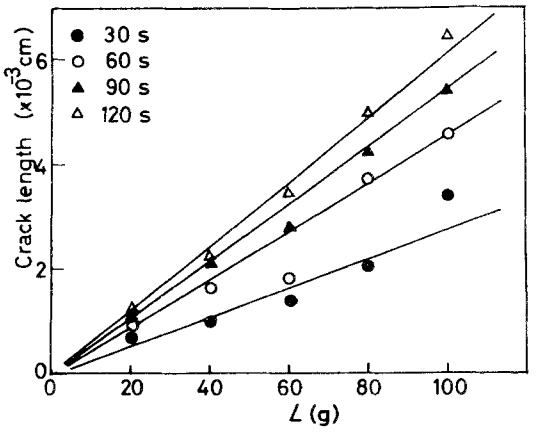

Figure 5 Plots of crack length against load, *L*.

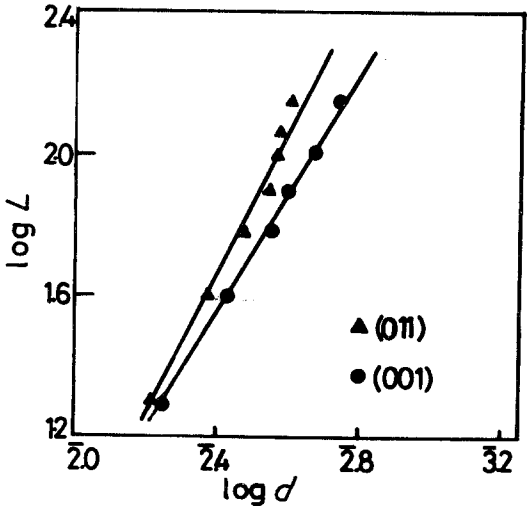

Figure 6 Plot of log L against log d for the two planes.

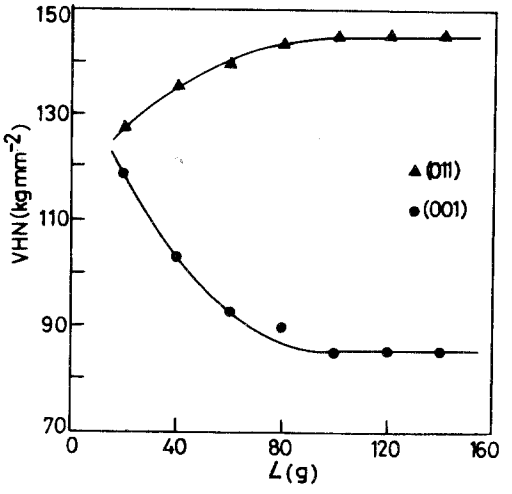

Figure 7 Plots of Vickers hardness number, VHN, against applied load L.

the deformation zone on loading is unknown, a rigorous analysis of lateral cracking is not possible. We have also observed material abrasion, or material chipping, such as df, as shown in Fig. 2. This may be attributed to intersection of median and lateral vents and is evident from the appearance of the discharged fragment. The subsurface damage, in agreement with the concept of Hagan and Swain [14], appears to consist of a heavy network of shear flow lines which represent the stages of crushing of the material into fine powder. Further, along with the Palmqvist cracks, a system of cracks reflecting the symmetry of the plastic indents were also observed, as marked cz in Fig. 1. Such bands of cracks, or annuli, extend into the indent from the edge and are always terminated by a crack free zone (cf), as marked in Figs. 1 and 2. These surface cracks are probably produced by elastic contact stresses at the specimen indenter surface, as pointed out by Hagan and Swain [14, 15].

On the other hand, the bulk cracks developed on the (001) planes, shown in Fig. 3, seem to emanate from the edges and corners of the indentation pit. Interestingly, unlike that on (011) faces, piling up of the material around the mark on (001) planes is an additional feature of surface observation. The formation of the observed median cracks may possibly be due to interaction of shear deformation flow lines beneath the indenter [14].

To characterize better the specimen, in so far as their micromechanical properties are concerned, the plot of log load, L, against log diagonal length, d, was established (Fig. 6). They yield straight lines in the investigated region, have slopes of $n \simeq 2.15$ and 1.65 for (011) and (001) planes respectively. Also, the variation of VHN with load for the two sets of planes is shown in Fig. 7. A marked difference in the observed VHN values for the two planes is noteworthy. In the case of (011) planes the VHN increases gradually up to 80 g and remains constant thereafter. On the contrary, (001) planes exhibit, before saturation, gradual decrease in VHN up to around 80 g. These variations support the concept of Onitsch [13], that if $n < 2$ the hardness number increases with decreasing load, and if $n > 2$ it decreases as the load is decreased. The load-independent hardness values differ from plane to plane, and in the present case they are $VHN_{(011)} = 144.96$ kg mm^{-2}, $VHN_{(001)} = 85.4$ kg mm^{-2}. Obviously, $VHN_{(011)} > VHN_{(001)}$ by 58.9%.

The observed anisotropy in hardness may be understood in terms of surface cracking and material erosion at the indentation mark. For indents on (001) faces, enough displaced material in addition to cracking, is found to have piled up around the edges and corners of the pit, as is evident from Fig. 3. Such displaced material is responsible for the observed variation in hardness, since the material at the corners will lead to measured increases in the diagonal lengths. This effect has also been observed by McColm and Wilson [20] on certain cubic bronzes. It appears that such a situation prevails up to 80 g of load. The observation that the VHN is independent of load beyond 80 g may be attributed to the fact that

when the depth of the diamond pyramid is much increased, the effect of the distorted zone beneath the indenter becomes much less prominent. But in the case of (0 1 1) faces, no piling up of the material is observed along the edges and corners of the indented figure, and hence in spite of the slight cracking and chipping the indentation diagonals are well defined. This supports the relatively soft nature of (001) cleavage planes as compared to the habit faces of the crystals, as observed.

Moreover, the observed gradual enhancement of VHN before 80 g of load is understandable if one considers the effect of the surface layers of the crystal. During the process of indentation, the impression of the diamond pyramid may penetrate to a depth comparable with or greater than the thickness of the surface layer. Since this layer is pierced by the indenter, its effect will be marked at low loads. Consequently, the noticeable increase in VHN on the (0 1 1) planes is observed. Beyond 80 g, when the impression reaches a depth at which the undistorted layer of the material exists, the microhardness ceases to depend on loading.

It may, however, be noted that both the crack velocity and the VHN on (0 1 1) planes follow an identical variation with load; their values increase linearly up to 80 g load. This suggests a close relation between the two micromechanical quantities with greater indenter loads, when the hardness shows increasing trend, the indentation induced cracks propagate faster, before attaining a steady load-independent value. The micromechanical characteristics of $BaMoO_4$ can therefore be indicated by either crack velocities or Vickers hardness. The amount of anisotropy in VHN with regard to the crystal planes can, however, be attributed as suggested by Armstrong and Raghuram [21], to the possible difference in the inclination of glide planes that accommodate dislocation motion during indentation. The larger the angle of inclination, the larger will be the microhardness as conceived by Boyarskaya and co-workers [22–24].

4. Conclusions

1. Surface cracking around the indentation-induced impression is observed both on the grown and the cleavage planes.

2. Unlike the cleavage plane, the habit face exhibits material chipping off, which is an early stage of material crushing and powdering. This suggests the interaction of heavily worked flow lines forming a tangled mesh beneath and around the deforming indenter.

3. The crack velocity tends to increase with applied loading and to saturate at 80 g.

4. The as-grown (0 1 1) faces have been found to be much harder than the (001) cleavage faces.

5. Large anisotropy in VHN with respect to crystal planes is noteworthy. Though the behaviour is different for the initial smaller values of the applied load, the indentation on the as-grown and cleavage planes resulted in a region where the VHN is not a function of the applied load.

6. The possible difference in the angles of intersections of glide planes might probably result in the hardness anisotropy.

Acknowledgements

One of us (GSTR) would like to thank CSIR, New Delhi, for the award of a Senior Research fellowship.

References

1. H. BÜCKLE, *Mater. Rev.* **4** (1959) 49.
2. *Idem*, "L'essai de Microdureté et ses Applications" (Publication Scientifiques et Techniques due Ministère de L'Air, Paris, 1960).
3. C. A. BROOKES and P. GREEN, *Nat. Phys. Sci.* **246** (1973) 246.
4. C. A. BROOKES and B. MOXLEY, *J. Phys. E: Sci. Instrum.* **8** (1975) 456.
5. E. H. L. J. DEKKER and G. D. RIECK, *J. Mater. Sci.* **9** (1974) 1839.
6. Y. J. KUMASHIRE, A. ITOH, T. KINOSHITA and M. SOBAJINA, *J. Mater. Sci.* **12** (1977) 595.
7. S. K. ARORA, T. ABRAHAM, G. S. TRIVIKRAMA RAO and R. S. GODBOLE, *ibid.* **17** (1982) 2825.
8. D. TABOR, "The Hardness of Metals" (Clarendon Press, Oxford, 1951).
9. S. K. ARORA and G. S. TRIVIKRAMA RAO, *J. Crystal Growth* **53** (1981) 627.
10. R. W. G. WYCOFF, "Crystal Structure" (Interscience Publishing Inc., New York, 1951) p. 151.
11. S. K. ARORA and G. S. TRIVIKRAMA RAO, *Cryst. Res. Technol.* **17** (1982) 1303.
12. S. K. ARORA, G. S. TRIVIKRAMA RAO and M. S. SETTY, *Indian J. Pure Appl. Phys.* **20** (1982) 733.
13. E. M. ONITSCH, *Mikroskopie* **2** (1947) 131.
14. J. T. HAGAN and M. V. SWAIN, *J. Phys. D: Appl. Phys.* **11** (1978) 2091.
15. M. V. SWAIN and J. T. HAGAN, *ibid.* 9 (1976) 2201.
16. S. PALMQVIST, *Jernkontorets Ann.* **141** (1957) 300.
17. *Idem*, *Arch. Eisenlwettenw.* **33** (1962) 29.
18. I. M. OGILVY, C. M. PERROT and J. N. SUITER, *Wear* **43** (1977) 239.
19. B. R. LAWN and R. WILSHAW, *J. Mater. Sci.* **10**

(1975) 1049.
20. I. J. McCOLM and S. J. WILSON, *J. Solid State Chem.* **26** (1978) 223.
21. R. W. ARMSTRONG and A. C. RAGHURAM, in "The Science of Hardness Testing and its Research Applications", edited by J. Westbrook and H. Conrad (American Society for Metals, Metals Park, Ohio, 1973) Chap. 13.
22. Yu. S. BOYARSKAYA and M. I. VALKOVSKYA, in "Sclerometry" (in Russian) (Nauka, Moscow, 1968) p. 153.
23. Yu. S. BOYARSKAYA and D. Z. GRABCO, *Krist. Technol.* **8** (1973) 1367.
24. C. A. BROOKES and R. H. BURNAND, in "The Science of Hardness Testing and its Research Applications", edited by J. Westbrook and H. Conrad, (American Society for Metals, Metals Park, Ohio, 1973) Chap. 15.

Received 13 December 1982
and accepted 19 May 1983